Titanium Scavenging in Ag-Cu-Ti Active Braze Joints

The scavenging mechanism was studied by brazing joints with elemental Fe, Ni, and Co spacers

BY P. T. VIANCO, J. J. STEPHENS, P. F. HLAVA, AND C. A. WALKER

ABSTRACT. Poor hermeticity was observed for Al_2O_3-Al_2O_3 braze joints using a Fe-29Ni-17Co alloy spacer and Ag-Cu-Ti active filler metal. Titanium was scavenged from the filler metal by formation of a (Fe, Ni, Co)-Ti "lacework" phase. The scavenging mechanism was further studied using braze joints made with elemental Fe, Ni, or Co spacers. The Fe spacer caused development of Fe_xTi_y phases at its interface but allowed a significant Ti_xO_y layer to form at the Ag-Cu-Ti/Al_2O_3 interface, resulting in 100% hermetic joints. The Co spacer caused a lacework phase and only intermittent Ti_xO_y reaction layer at the Ag-Cu-Ti/Al_2O_3 interface; 75% of the buttons were hermetic. The Ni spacer caused extensive scavenging of Ti, resulting in an absence of a Ti_xO_y layer at the Ag-Cu-Ti/Al_2O_3 interface and no hermetic joints. Braze joint mechanical strength correlated primarily with the presence or absence of the Ti_xO_y layer. The Fe, Ni, and Co spacer experiments suggested that lacework phase formation in Fe-29Ni-17Co/Ag-Cu-Ti joints was primarily a result of scavenging by the Ni and Co components of the spacer material. Mechanical strength behavior and poor hermeticity were commensurate with the absence of a Ti_xO_y reaction layer at the Ag-Cu-Ti/Al_2O_3 interface. An Fe or inactive metal barrier layer would provide a means to curtail the scavenging reaction.

Introduction

The properties of ceramic materials allow them to be suitable for applications from heat engines to electro-optical devices (Refs. 1, 2). Filler metal techniques (soldering and brazing) have been used to successfully join metals and ceramics. Metallization layers or active filler metals are required to promote the necessary wetting and spreading by the braze alloy over the ceramic surface (Ref. 3).

P. T. VIANCO, J. J. STEPHENS, P. F. HLAVA, and C. A. WALKER are with Sandia National Laboratories, Albuquerque, N.Mex.

Thermal expansion mismatch between metals and ceramics can generate damaging residual stresses within the joint (Ref. 4). Those stresses can be reduced by selecting a metal alloy having a thermal expansion coefficient that closely matches that of the ceramic material. For example, the thermal expansion coefficient of the Fe-Ni-Co alloy, Kovar™ (Fe-29Ni-17Co, wt-%), is 6.2 ppm/°C (25–500°C) and is well matched to that of alumina (Al_2O_3), 7–9 ppm/°C (Refs. 4–6). An active filler metal for metal-ceramic joining is the 63.3Ag-35.1Cu-1.6Ti composition (Cusil ABA™, Ref. 7). It is based upon the eutectic Ag-Cu alloy (72Ag-28Cu, $T_{eut.}$ = 780°C) with Ti serving as the active element to promote wetting of the bare Al_2O_3 surface.

A particular application required that two pieces of Al_2O_3 be joined together with an Fe-29Ni-17Co alloy interlayer or spacer between them. Test specimens, based upon the ASTM F-19 "tensile button" configuration, were brazed with the Ag-Cu-Ti active filler metal. The prototype braze joints exhibited satisfactory strength, but did not satisfy hermeticity requirements. Optical micrographs of the braze joint made at 850°C (1562°F) for 5 min are shown in Fig. 1. A lacework structure developed within the filler metal (Fig. 1A). The layer ranged from 1–3 μm thick. No Ti-based reaction layer, designated Ti_xO_y, formed at the Ag-Cu-Ti/Al_2O_3 interface — Fig. 1B. By comparison, A_2O_3/Al_2O_3 braze joints made under the same process conditions, but in the absence of a Fe-29Ni-17Co spacer, exhibited no lacework phase in the filler metal (Fig. 2A) and developed a 1.92±0.38-μm-thick Ti_xO_y reaction layer at the Ag-Cu-Ti/Al_2O_3 interfaces — Fig. 2B. For this latter case, a theoretical Ti_xO_y thickness was calculated to be 1.7 μm at each interface, assuming a filler metal thickness of 51 μm and a TiO stoichiometry (Ref. 6).

KEY WORDS

Brazing
Active Filler Metals
Titanium
Scavenging
Ceramic Materials

Electron microprobe analysis (EMPA) identified Fe, Co, Ni, Cu, and Ti in the lacework phase. Two compositional variations were measured, one richer in Fe and the second richer in Ni. The Fe-rich composition occurred when the lacework phase was located near the Fe-29Ni-17Co spacer. This case is represented by location A in the scanning electron microscope (SEM) photograph in Fig. 3 (backscattered electron or BSE mode). When the phase was located further into the filler metal (location B), a Ni-rich composition was observed. Electron microprobe analysis determined the composition of the Fe-rich phase to be (at-%) Ti, 30%; Fe, 46%; Ni, 10.1%; Co, 12.2%; Cu, 1.2%; and Ag, 0.5%. The Fe, Co, Ni, and Cu elements were combined and compared against the Ti content. (Silver was assumed to have had little role in the phase composition.) The Ni, Co, and Cu concentrations were normalized to the Fe content (that is, the Fe concentration equaled unity). The resulting stoichiometry was $(Fe_{1.0}Ni_{0.23}Co_{0.27}Cu_{0.03})_{2.3}Ti$. The composition of the Ni-rich sublayer was Ti, 24%; Fe, 6.7%; Ni, 48.4%; Co, 8.4%; Cu, 12.3%; and Ag, 0.2%. Normalized to the Ni content, this composition was represented as $(Fe_{0.14}Ni_{1.0}Co_{0.17}Cu_{0.25})_3Ti$.

The EMPA evaluation detected only a slight, intermittent Ti signal at the Ag-Cu-Ti/Al_2O_3 interface, confirming the absence of a significant Ti_xO_y reaction layer. Also, there was no appreciable Ti remaining within the filler metal.

The above analyses suggest the following scenario. The scavenging process began by the Ti component of the filler metal reacting at the Fe-29Ni-17Co spacer

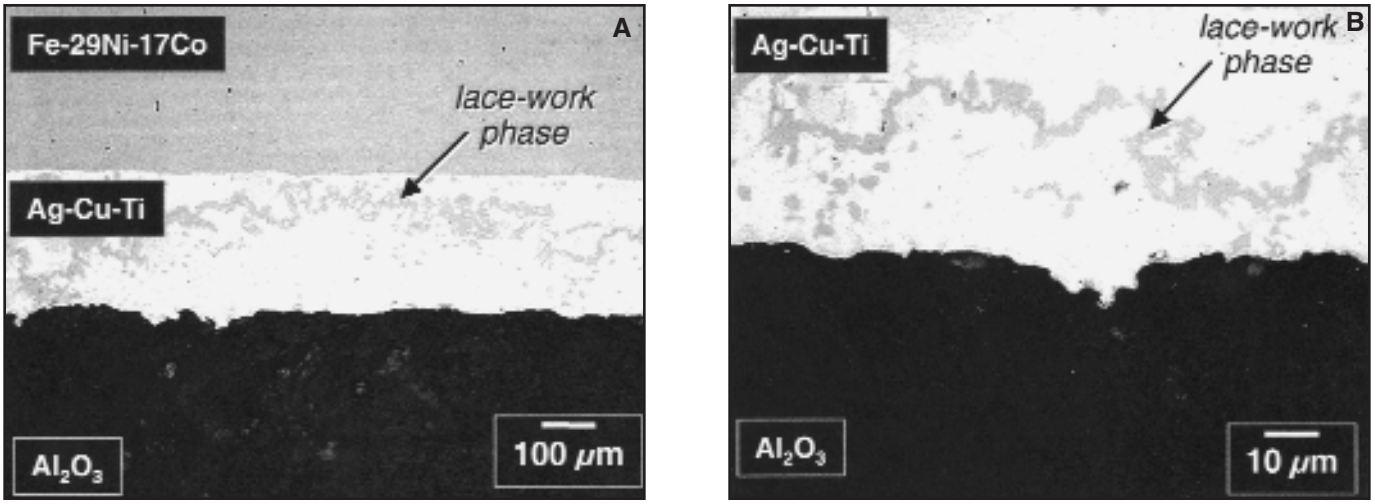

Fig. 1 — A — Optical micrograph of an Al_2O_3/Al_2O_3 joint made with a Fe-29Ni-17Co spacer showing the lacework phase. The filler metal was the Ag-Cu-Ti alloy; B — high-magnification optical micrograph of the Ag-Cu-Ti/Al_2O_3 interface confirming the absence of a Ti_xO_y reaction layer. The process conditions were 850°C and 5 min.

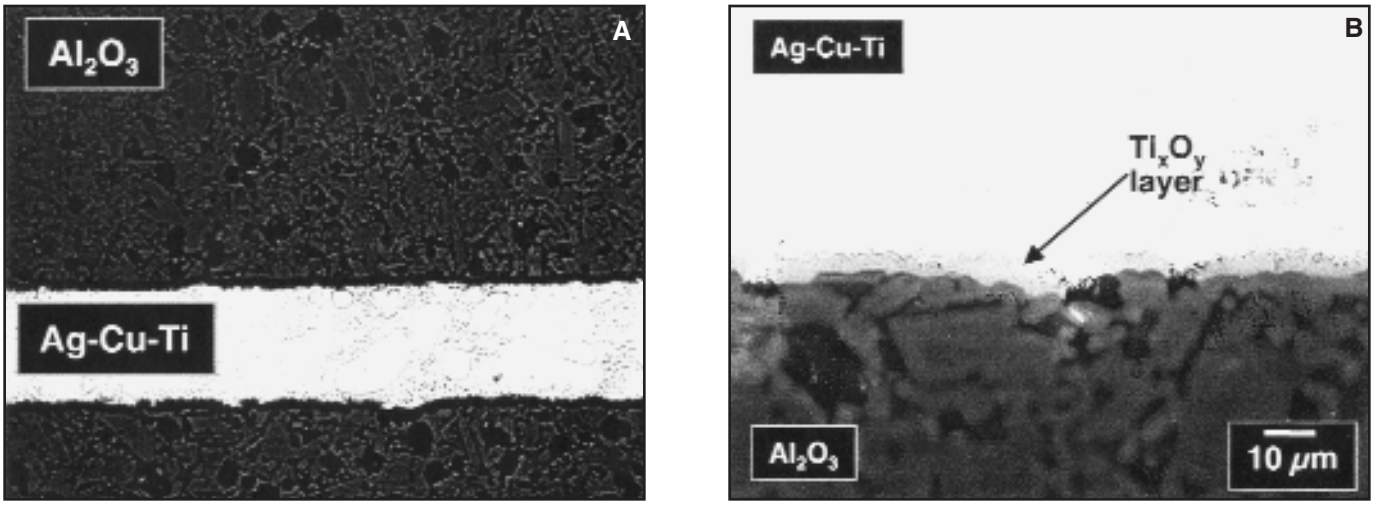

Fig. 2 — A — Optical micrographs of the Al_2O_3/Al_2O_3 joint made with Ag-Cu-Ti filler metal (no spacer). The filler metal was the Ag-Cu-Ti alloy. No lacework phase was present; B — high-magnification optical micrograph of the Ag-Cu-Ti/Al_2O_3 interface showing a thick Ti_xO_y reaction layer. The process conditions were 850°C and 5 min.

interface, forming the Fe-rich lacework phase. Then, the lacework phase developed further, becoming Ni-rich and separating from the Ag-Cu-Ti/Fe-29Ni-17Co interface. It remained located in the molten braze alloy through solidification. These reactions prevented Ti from diffusing to, and reacting at, the Ag-Cu-Ti/Al_2O_3 interface.

A similar scavenging reaction was observed by Hahn, Kim, and Kang for Al_2O_3/Fe-38.2Ni-13.0Co-4.7Nb-1.5Ti-0.03Al (Inconel 909™) braze joints made with the same Ag-Cu-Ti filler metal (Refs. 8, 9). The layer contained Fe, Ni, Co, and Ti and was located along the Ag-Cu-Ti/Fe-Ni-Co interface. A thin reaction layer formed at the Cu-Ag-Ti/Al_2O_3 interface, containing Ti as well as traces of Fe, Ni, and Co. No quantitative compositional determinations were made by the authors.

Wielage, Podlesak, and Klose examined a reaction layer that formed between the Ag-27Cu-3Ti filler metal and an Fe-Ni-Co alloy substrate (Ref. 10). A meandering, lacework reaction layer was located near the substrate interface. Two compositions were recorded. The approximately 1-μm-thick layer closest to the Fe-Ni-Co base alloy had the stoichiometry (at-%) of Ti, 26%; Fe, 48%; Ni, 11%; Co, 15%; there was no appreciable Cu or Ag content. The second composition (of the approximately 2-μm-thick layer) had the stoichiometry (at-%): Ti, 22%; Fe, 13%; Ni, 47%; Co, 10%; Cu, 8%; there was no appreciable Ag in this phase. Both compositions are very similar to those observed in the present study.

In the study described here, the scavenging process that occurred between the Ag-Cu-Ti active braze filler metal and the Fe-29Ni-17Co metal alloy was further studied by evaluating Al_2O_3 to Al_2O_3 braze joints made with the same Ag-Cu-Ti filler metal, but using 100% Fe, Ni, or Co spacers in place of the Fe-29Ni-17Co alloy. The objective was to determine the extent to which each the three primary elements in the alloy — Fe, Ni, or Co — had a role in the scavenging process. The specific information gathered in this study would be of value to design engineers wishing to use active braze alloys to join ceramics to this and other Fe-, Ni-, or Co-containing metal alloys. These data also demonstrate the magnitude of potential interactions that can occur in the complex materials systems that characterize metal-ceramic braze joints. After all, some de-

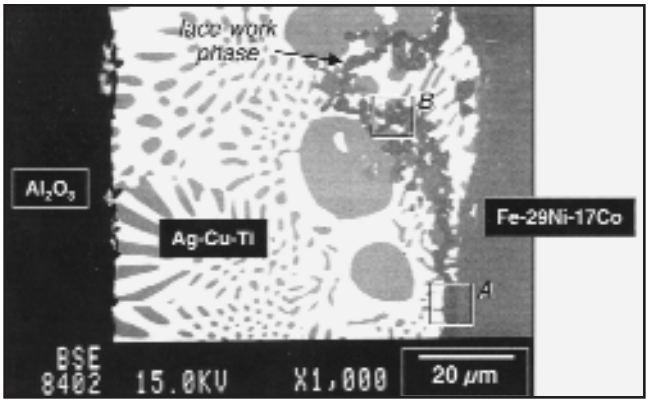

Fig. 3 — Scanning electron micrograph (back-scattered electron or BSE) showing the lacework phase in the Fe-29Ni-17Co/Ag-Cu-Ti/Al_2O_3 braze joint and the two locations A and B evaluated by EMPA.

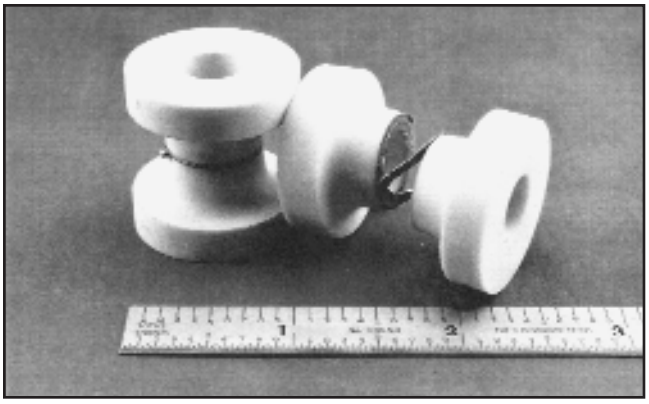

Fig. 4 — Stereo photograph of the ASTM-F19 tensile button specimen. The spacer can be observed between the two Al_2O_3 parts.

gree of base metal dissolution occurs in nearly all brazed joints. Moreover, the fact that the active element (Ti), which has such a crucial role in the successful performance of the joint, is present at such low concentrations implies that it being scavenged can significantly impact the performance of the braze joint.

Experimental Procedures

Test Specimens

The alumina substrates were obtained in the ASTM F19 "tensile button" configuration and made of Wesgo™ AL500 alumina (Ref. 11). The specimen is shown in Fig. 4. The buttons were air fired at 1575°C for two hours prior to the brazing cycle. The Fe, Ni, and Co spacers were punched from sheet stock. The Ni-spacer thickness was 0.127 mm (0.005 in.) while the thicknesses of the Fe and Co spacers were 0.254 mm (0.010 in.). The surfaces were degreased prior to assembly. The braze joint was constructed by placing a spacer between the minor diameters of two Al_2O_3 buttons. Then, a 54-μm (0.002-in.) -thick foil of the 63.3Ag-35.1Cu-1.6Ti (Cusil ABA™) filler metal was located at each of the two Fe-29Ni-17Co/Al_2O_3 junctures.

Process Parameters

The braze joints were fabricated in a resistance furnace according to the following general furnace schedule:

25°C–730°C; 10°C/min ramp
730°C, 15 min hold
730°C–T_p; 5°C/min ramp
T_p, t_p hold
T_p–730°C, 10°C/min ramp
730°C–25°C, furnace cooling ramp.

The peak temperature/time (T_p/t_p) combinations were 850°C (1562°F), 5 min and 900°C (1652°F), 10 min. An Ar partial pressure of 1.0–1.5 torr atmosphere was used during the brazing processes.

Sample Analysis

Upon completion of the fabrication step, each braze joint was evaluated for hermeticity using commercial He leak detection equipment. A joint was considered to be hermetic when the leak rate was less than 10^{-9} atm-cc/s.

The tensile strength of the braze joints was measured. Testing in tension was preferred to a shear test because of its greater sensitivity to the overall microstructure of the filler metal joint, which includes the base material, the filler metal, the reaction layers, and the interfaces between these various structures. By comparison, a great deal of this information is lost in a shear test. For example, the localized shear stresses do not as readily reveal the susceptibility of interfaces to failure. Also, the fracture surfaces can be severely degraded as the surfaces slide past one another. It was understood that tension testing of a filler metal joint will produce a greater data scatter. So, particular care was taken to minimize variations due to experimental technique. Finally, it is important to document the tensile strength/fracture behavior of these braze joints because they will be exposed to tensile stress in engineering applications, either through an applied load or by residual stresses.

The strength of the braze joints was measured on a servo hydraulic load frame using a crosshead displacement rate of 10 mm/min. A minimum of three tensile button samples were tested per experimental condition. The maximum tensile load was converted to a maximum tensile stress; an overall strength value was represented as the mean and ± one standard deviation of the individual test. The fracture surfaces of each sample were examined for the extent of the failure modes that were present.

The thickness of the Ti_xO_y reaction layer was measured at the filler metal/Al_2O_3 interface. The measurements were made from 1000⟨ optical micrographs. Six measurements were performed from a minimum of two separate micrographs. The data were represented as a mean and ±one standard deviation.

Electron microprobe analysis (EMPA) was used to investigate distribution of elements within the braze joints. The appropriate materials standards and calibration practices were followed prior to each analysis. The EMPA traces were compiled from spot analyses taken at 1-μm increments across the braze joints, perpendicular to the interface. Fourteen such traces were performed per each test specimen. The recorded elements were Ag, Cu, Ti, X (X = Fe, NI, or Co), Al, and Si. The machine was operated at an accelerating voltage of 15 kV, resulting in X-ray sampling volume with a 1–2-μm projected diameter.

Results

Ag-Cu-Ti Filler Metal Interactions with the Fe Spacer Material

Shown in Fig. 5 is an optical micrograph of the braze joint made with an Fe spacer and the 850°C, 5-min brazing process. Some runout of the filler metal reduced the joint thickness to approximately 20 μm; the excessive runout was particular only to the Fe spacer material. The lacework phase was absent from the filler metal. The image did not distinguish a reaction layer at the Ag-Cu-Ti/Fe interface. A significant Ti_xO_y reaction layer formed at the Ag-Cu-Ti/Al_2O_3 interface, having a thickness of 2.27±0.64 μm. This thickness was less than the 3.4-μm value predicted by theoretical calculation (which assumed a TiO stoichiometry), or the 3.8-μm thickness measured from Al_2O_3/Al_2O_3 joints (see Introduction). This discrepancy could not be conclusively attributed to filler metal runout. Also, the absence or presence of a reaction layer at the Ag-Cu-Ti/Fe interface had not been

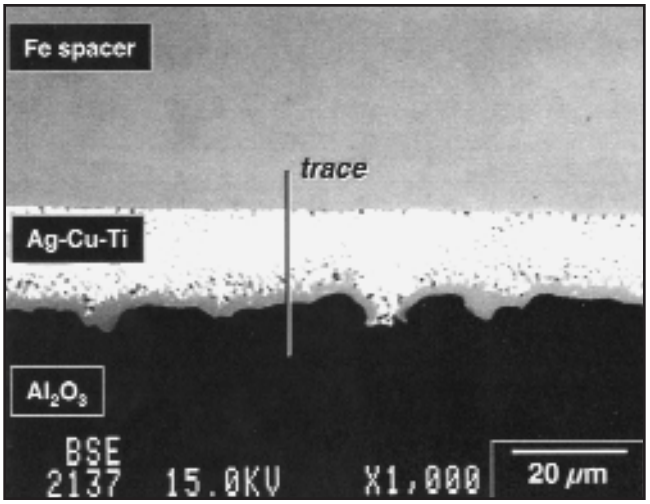

Fig. 5 — SEM photograph (BSE) of the braze joint formed between the Fe spacer and the Al_2O_3 substrate. The brazing process was 850°C and 5 min.

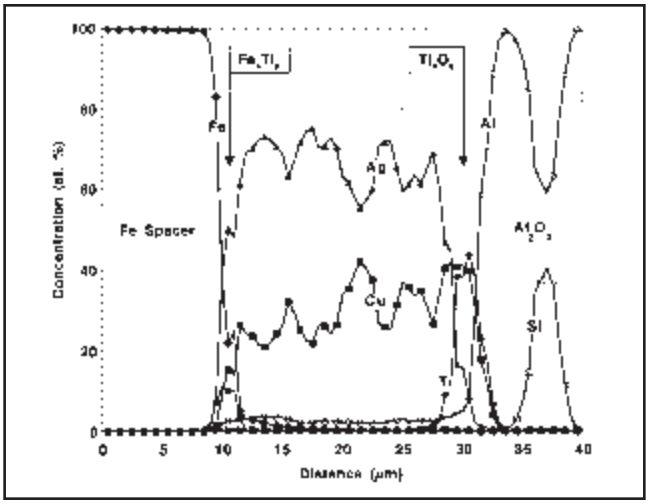

Fig. 6 — Electron microprobe analysis trace across the braze joint between the Fe spacer and the Al_2O_3 substrate. The brazing process was 850°C and 5 min.

determined by EMPA. The process condition of 900°C, 10 min produced a similarly configured braze joint; a slightly greater, mean Ti_xO_y layer thickness was measured (2.44±0.54 μm).

Shown in Fig. 6 is an EMPA analysis from a trace across the braze joint made with the 850°C, 5-min process. Only one-half of the experimental data points (symbols) have been included in this and subsequent EMPA traces for clarity. The compositional profile was also representative of the 900°C (1652°F), 10-min process. The Ag content of the filler metal generally increased, and the Cu levels decreased, from the Al_2O_3 side of the joint toward the Fe spacer.

Trace levels of Ti were also observed in the filler metal; midpoint concentrations were 0.5±1.1 at-% after processing at 850°C for 5 min and 0.4±0.5 at-% following the 900°C, 10-min process.

There was a persistent concentration of Al in the filler metal. The values measured at the midpoint of the joint were 3.2±0.7 at-% after the 850°C, 5-min process and 3.4±1.5 μm following the 900°C, 10-min process. There were no correlations between the Al concentration and the concentrations of the other elements. The presence of Al in the filler metal was likely a product of the reduction-oxidation reaction between Ti and Al that resulted in the Ti_xO_y layer at the Ag-Cu-Ti/Al_2O_3 interface (see discussion below). The absence of a significant Si signal (the glass binder of the Al_2O_3 ceramic) indicated that Al in the filler metal was not caused by a physical breakup of the ceramic.

The composition of the Ti_xO_y reaction layer at the Ag-Cu-Ti/Al_2O_3 interface was examined. Reproducible concentrations of Ti as well as Cu, Ag, Al, and Si were present for either processing condition (Table 1). The equipment did not detect O_2. The presence of Cu and Al may represent the formation of the more complex $Cu_x(Ti,Al)_yO_z$ reaction product such as the $Cu_2(Ti,Al)_4O$ composition reported by A. Moorehead et al. (Ref. 12). The concentrations in Table 1 did not coincide with this composition. If the Al signal was excluded from the analysis, then a $Cu_xTi_yO_z$ reaction product would be predicted, having a stoichiometry similar to the Ti_3Cu_3O reaction layer observed by Bang and Liu in braze joints made between a Cu-Ti filler metal and Al_2O_3 (Ref. 13). The presence of Ag in Table 1 was not observed in the reaction layers cited from prior studies of the Ag-Cu-Ti/Al_2O_3 system as listed in Ref. 13.

Table 1 — Elemental Concentrations at the Ag-Cu-Ti/Al_2O_3 Interface as a Function of Process Conditions for Braze Joints with an Fe Spacer

	Elemental Concentrations (at-%)				
Process Conditions	Ti	Cu	Ag	Al	Si
850°C, 5 min	45 ± 2	39 ± 3	7 ± 5	7 ± 3	0.5 ± 0.8
900°C, 10 min	48 ± 4	36 ± 6	6 ± 6	10 ± 4	0.2 ± 0.6

The EMPA trace did identify a reaction layer at the Ag-Cu-Ti/Fe interface. The elements Ag, Cu, Ti, Al, and Fe were present; Si was absent. Aluminum was detected at levels slightly above those observed in the interior of the gap. The compositional data are provided in Table 2. The elemental concentrations fell into two mutually exclusive compositions designated A and B, which were distinguished by Cu levels. For the 850°C, 5-min process, the A and B compositions had Cu levels of 21±3 at-% and 4±1 at-%, respectively, and occurred with equal frequency (N = 7 of 14 traces). The different Cu levels between A and B groups were compensated by the Ag content; only small changes occurred to the concentrations of the other elements.

In the case of the 900°C, 10-min process, the Cu concentrations also distinguished the two composition groups A and B. However, the difference in Cu concentrations were compensated by the Ti and Fe concentrations rather than by the Ag levels. The Ti contents of both groups A and B were higher than the respective values measured for the 850°C process. The B composition was more prevalent, being observed in 11 of the 14 EMPA traces. The small amount of Ti scavenged by the Fe spacer to form the interface reaction layer was likely responsible for the Ti_xO_y layer thickness at the Ag-Cu-Ti/Al_2O_3 interface being less than predicted values.

The Fe signal dropped off rapidly away from the Ag-Cu-Ti/Fe interface. The Fe concentrations at the trace (joint) midpoints were 0.4±0.3 at-% for the 850°C, 5-min process and 1.3±0.8 at-% for the 900°C, 10 min. These low Fe contents represented a supersaturated, solid-solution retained from the finite solubility of Fe in Ag and in Cu (3–5 at-% each) at a reference temperature of 800°C (Ref. 14).

The data in Table 2 were analyzed for phase stoichiometries beginning with the

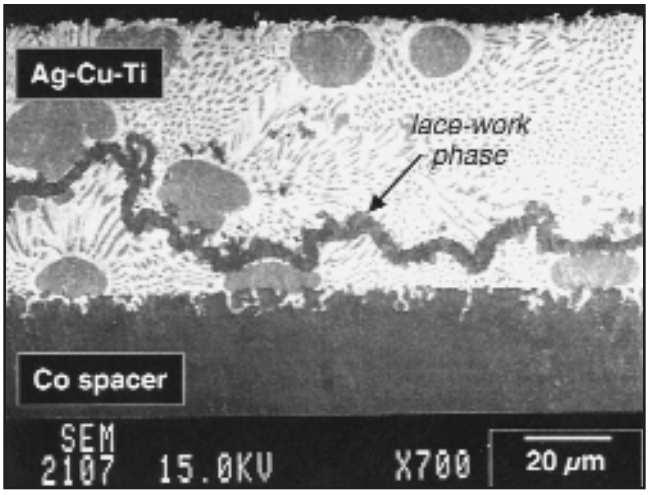

Fig. 7 — SEM (SE) photograph showing the lacework phase in the braze joint formed with the Co spacer, using the 850°C, 5-min brazing process.

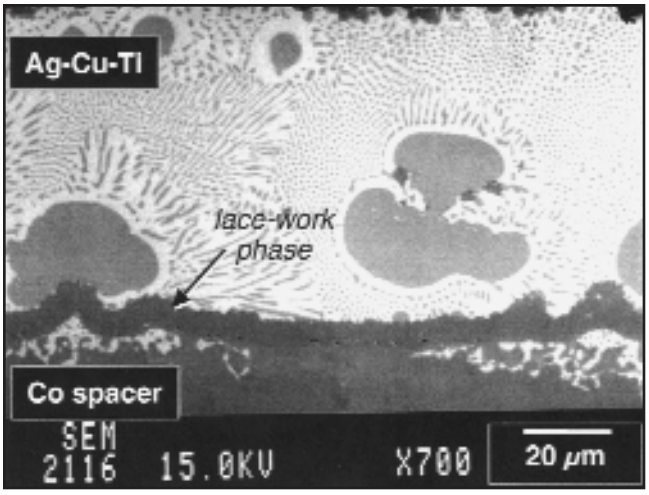

Fig. 8 — SEM photograph of the braze joint made with the Co spacer, using the 900°C, 10-min. process conditions.

Table 2 — Elemental Concentrations at the Ag-Cu-Ti/Fe Interface

Process Conditions		Elemental Concentrations (at-%) Ti	Cu	Ag	Fe	Al
850°C, 5 min	A (N=7)	9 ± 2	21 ± 13	36 ± 8	36 ± 9	3 ± 1
	B (N=7)	11 ± 2	4 ± 1	44 ± 6	38 ± 6	1.1 ± 0.7
900°C, 10 min	A (N=3)	18 ± 6	23 ± 11	33 ± 16	26 ± 20	2.7 ± 0.6
	B (N=11)	27 ± 7	4 ± 2	27 ± 12	40 ± 17	2 ± 1

850°C, 5-min process. The relatively small Al concentration was not considered. The Ag signal was not taken into account because its source was likely the X-ray sampling volume striking the nearby filler metal field. The latter phenomenon would also explain the high and low Cu contents that distinguished groups A and B for either process condition.

Therefore, it was assumed that the reaction layers for both groups were comprised entirely of Fe and Ti. The same (normalized) stoichiometry was computed for both A and B compositions, namely Fe_4Ti. The equilibrium binary phase diagram for the Fe-Ti system does not indicate an Fe_4Ti compound (Ref. 15). However, it is not unusual for interface reactions to produce metastable phases that are not present on the equilibrium phase diagram (Refs. 16–18). On the other hand, the Fe_4Ti stoichiometry may represent a mixture of documented equilibrium phases, for example, the combination of Fe_2Ti (87%) and (α)Fe (13%).

In the case of the 900°C, 10-min process, the quantitative trends were different. The group B reaction composition was more prevalent, found in 11 of 14 traces. The Al and Ag contents were similar between the two phase compositions. The Fe and Ti concentrations of both A and B compositions had a similar stoichiometry of Fe_3Ti_2. The equilibrium Fe-Ti binary alloy phase diagram does not exhibit such a line compound (Ref. 15). Therefore, either the Fe_3Ti_2 stoichiometry represented a metastable phase or it indicated a mixture of the FeTi (35%) and Fe_2Ti (65%) equilibrium phases.

The presence of the Ti_xO_y reaction layer at the Ag-Cu-Ti/Al_2O_3 interface coincided with all of the braze joints being hermetic.

The pull strength of samples made at 850°C and 5 min was 80±55 MPa (12±8 ksi). Ninety-three percent of the fracture path was in the Al_2O_3; the remaining 7% was along the Ag-Cu-Ti/Al_2O_3 interface. This strength exceeds that of similarly processed Al_2O_3/Ag-Cu-Ti/Al_2O_3 joints made without a spacer (64±4 MPa, 9.4±0.6 ksi), or joints made with the Fe-29Ni-17Co spacer (41±11 MPa, 6±2 ksi).

The joints made with the 900°C, 10-min process exhibited lower strengths of 51±15 MPa (7±2 ksi). This strength is the same as similarly processed braze joints using the Fe-29Ni-17Co spacer (53±14 MPa, 8±2 ksi), which did not produce a Ti_xO_y reaction layer. Approximately 70% of the fracture path was in the Al_2O_3 material; the remainder was along the Ag-Cu-Ti/Al_2O_3 interface indicating a weakening of the latter interface. A slightly thicker Ti_xO_y reaction layer was observed after the 900°C, 10-min process (2.44±0.54 μm) vs. the 850°C, 5-min process (2.27±0.64 μm). Studies by Scott et al. have indicated that the strength of active braze joints can reach a maximum as a function of reaction layer thickness (Ref. 19). A thickness beyond that maximum value results in a strength decrease due to the greater likelihood of flaws in the layer structure that facilitate crack initiation. Such a scenario may explain the above strength data.

Ag-Cu-Ti Filler Metal Interactions with the Co Spacer Material

A lacework phase was observed in the braze joints made to the Co spacer. Shown in Figs. 7 and 8 are SEM (secondary emission or SE) photographs of the lacework phase after the 850°C, 5-min and 900°C, 10-min processes, respectively. In general, the lacework phase was more toward the interior of the filler with the 850°C, 5-min process conditions and closer to the Co spacer for joints made with the 900°C, 10-min process. The phase thickness ranged from 3.5 to 4.5 μm. The morphology of the phase, particularly as illustrated in Fig. 8, indicated that it formed at, and subsequently moved away from, the Ag-Cu-Ti/Co interface prior to solidification. Considerable filler metal infiltration into the Co spacer grain boundaries (Figs. 7 and 8) indicated that dissolution of the Co spacer into the molten filler metal had occurred after formation of the lacework phase. A widely scattered Ti_xO_y reaction layer was observed for both processes; it measured 0.56±0.49 μm thick after the 850°C, 5-min process and 0.90±1.1 μm following the 900°C, 10-min process.

The EMPA trace in Fig. 9 (850°C, 5 min) shows the case for which the lace-

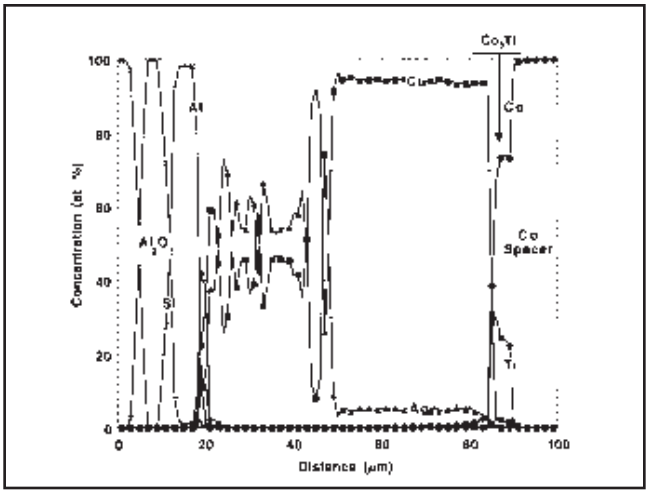

Fig. 9 — Electron microprobe analysis trace across the Ag-Cu-Ti/Co braze joint processed at 850°C for 5 min. The lacework phase was a reaction layer at the Ag-Cu-Ti/Co interface.

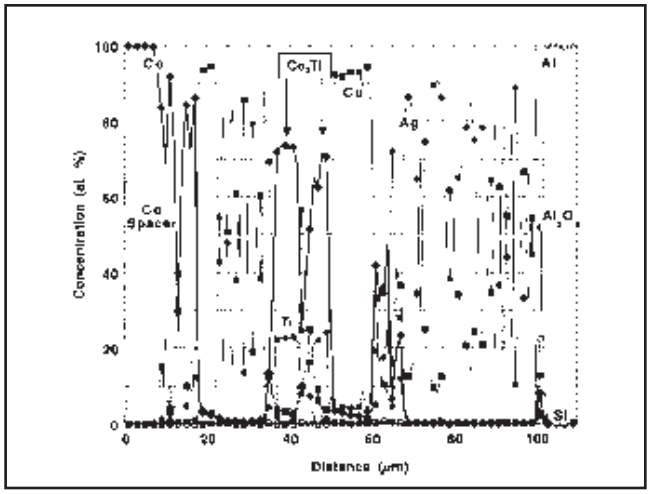

Fig. 10 — Electron microprobe analysis trace across the Ag-Cu-Ti/Co braze joint processed at 850°C for 5 min. The lacework phase is located in the interior of the filler metal.

work phase was still a reaction layer at the Ag-Cu-Ti/Co interface. When located here, the phase composition was always Co_3Ti, a stoichiometry that is observed in the equilibrium phase diagram (Ref. 20). The Co concentration quickly diminished away from the Ag-Cu-Ti/Co interface reaction layer; no Ti, Al, or Si signals were detected in the gap. The Cu and Ag concentrations exhibited profiles expected of the eutectic Ag-Cu binary composition.

The EMPA trace in Fig. 10 (850°C, 5-min process) shows the lacework phase when it was located in the interior of the filler metal. The trace intercepted the phase twice. The lacework phase in the interior of the joint exhibited two primary compositions designated as groups A and B. The two compositions, which were not mutually exclusive — that is, both could occur simultaneously in a single trace across the lacework phase — are listed in Table 3. The frequencies with which A and B compositions occurred were roughly equivalent under both process conditions. The A-phase composition, which was observed with both brazing processes, was the Co_3Ti stoichiometry. The presence of Cu in the layer was likely caused by a small mutual solubility between Cu and Co (1–3 at-% at 800°C) that was retained under supersaturation at the lower temperatures.

The B composition differed between the two process conditions (Table 3). The B composition for the 850°C, 5-min process showed a ratio of Cu to Ag representing the filler metal's baseline eutectic composition. The Ti and Co concentrations, normalized between one another, indicated a composition of Ti_3Co_4. This stoichiometry is not present in the binary alloy phase diagram; thus, it may represent a metastable phase or indicate a mixture of the equilibrium TiCo (77%) and $TiCo_2$ (23%) phases. The B composition recorded after the 900°C for 10-min process suggested the presence of primarily αCo (90%) and a small amount of Ti, possible as $TiCo_3$ (10%).

Table 3 — Elemental Concentrations of the Lacework Phase within the Gap of the Ag-Cu-Ti/Co Braze Joints

Process Conditions		Elemental Concentrations (at-%) Ti	Cu	Ag	Co
850°C, 5 min	A (N=6)	24 ± 1	4 ± 1	0.2 ± 0.3	72 ± 2
	B (N=5)	15 ± 9	25 ± 18	40 ± 22	20 ± 18
900°C, 10 min	A (N=6)	22 ± 1	3 ± 0	0.2 ± 0.4	74 ± 1
	B (N=6)	7 ± 2	4.2 ± 0.4	1 ± 2	88 ± 3

The EMPA traces in Figs. 9 and 10 also intersected the Ag-Cu-Ti/Al_2O_3 interface where a peak in the Ti signal indicated a Ti_xO_y reaction layer. In general, the Ti_xO_y reaction layers were relatively thin and intermittently present after either process condition. The layer composition following the 850°C, 5-min process was 23±13 at-% Ti, 12±9 at-% Co, 1.4±0.9 at-% Si; the balance was Al (64 at-%). Only trace amounts of Cu and Ag were observed. The process conditions of 900°C and 10 min resulted in a composition of 13±10 at-% Ti, 24±29 at-% Co, 2±4 at-% Si, and the balance Al (61 at-%). Silver and Cu contents were 5±4 at-% and 6±3 at-%, respectively. The limited layer thickness was likely responsible for the scatter in the composition data. Also, the Si and Al signals could have originated from the nearby Al_2O_3 substrate.

The more interesting finding about the Ag-Cu-Ti/Al_2O_3 interface reaction layer was the presence of Co. The individual EMPA traces were examined for their Ti and Co signals at this interface; the data are presented in Table 4. Two composition groups were observed that were mutually exclusive and of nearly equal frequency. Composition group A had high levels of Co and Ti. Group B was characterized by low concentrations of both elements and likely indicated locations of minimal reaction layer thickness. Therefore, specific to the group A composition, the 850°C, 5-min process caused a higher Ti concentration (36±6%) than Co (17±8%) while the 900°C, 10-min brazing process caused a higher Co concentration (54±16%) than Ti (23±4%).

Table 4 — Elemental Concentrations of Ti and Co at the Ag-Cu-Ti/Al_2O_3 Interface of Braze Joints Made with the Co Spacer

Process Conditions		Elemental Concentrations (at-%) Ti	Co
850°C, 5 min	A (N=8)	33 ± 6	17 ± 8
	B (N=6)	9 ± 3	6 ± 5
900°C, 10 min	A (N=6)	23 ± 4	54 ± 16
	B (N=8)	5 ± 4	1 ± 1

Hypotheses were considered to explain the presence of Co at the Ag-Cu-Ti/Al_2O_3 interface. It was not likely that the Co, which had dissolved into the molten filler metal, was physically entrapped in the re-

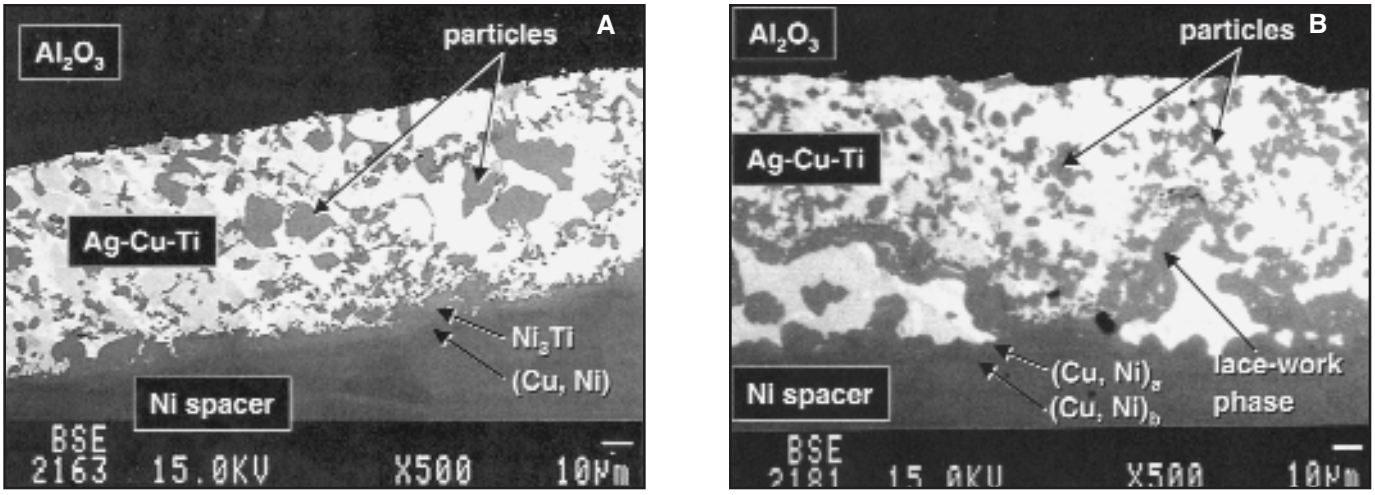

Fig. 11 — SEM (back-scattered electron) photographs of braze joint formed with the Ni spacer using the processing conditions: A — 850°C, 5 min; B — 900°C, 10 min.

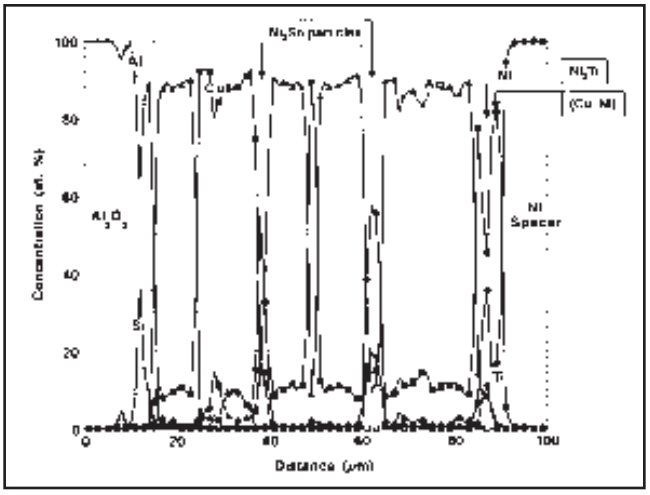

Fig. 12 — Electron microprobe analysis trace across the Ag-Cu-Ti/Ni braze joint processed at 850°C for 5 min.

action layer. The fact that neither Ag nor Cu showed such a tendency, given their far greater concentrations, discounted that scenario. Under the premise that Co was driven to the Ag-Cu-Ti/Al_2O_3 interface by a chemical potential, two possible mechanisms were considered. The first mechanism was that in which the Co competed with the Ti for a reduction-oxidation reaction with the Al_2O_3 substrate. The standard Gibbs free energy of formation calculations resulted in positive values at both 850°C and 900°C (Ref. 21)

$$3Co + Al_2O_3 \Rightarrow 2Al + 3CoO$$
$$\varnothing G = +207 \text{ kcal/mol (850°C)}$$
$$\varnothing G = +206 \text{ kcal/mol (900°C)} \quad (1)$$

indicating that thermodynamically, such reactions would not be spontaneous. However, as pointed out by Bang and Liu, a nonspontaneous reaction predicted from simply the *standard* Gibbs free energies of reaction may become spontaneous because oxygen and Al activities in the molten filler metal can cause the *total* Gibbs free energy to become negative (Ref. 13). (This is the very reason that the Ti/Al_2O_3 reduction-oxidation reaction occurs since, according to the standard Gibbs free energy calculation, this reaction should also be nonspontaneous.) An ancillary experiment was performed with a Co spacer and Cu-Ag eutectic filler metal, using the 900°C, 10-min process; it failed to produce an adherent joint. Also, there was no evidence of a reaction layer on the Al_2O_3 surface.

A second scenario was hypothesized in which the Ti_xO_y reduction-oxidation reaction proceeded initially. Then, a subsequent reduction-oxidation reaction took place between Co and the Ti_xO_y product. As was the case with the Ti/Al_2O_3 and Co/Al_2O_3 reactions, a positive *standard* Gibbs free energy of formation was calculated. But, as noted above, such a reaction may become spontaneous when the activities of Al and oxygen are taken into consideration.

Three of the four braze joints were hermetic; the less-than-perfect hermeticity was ascribed to the thinner, intermittent Ti_xO_y reaction layer.

The pull strength for samples made at 850°C and 5 min was 96±14 MPa (14±2 ksi). This value is well in excess of similarly processed, Al_2O_3/Ag-Cu-Ti/Al_2O_3 joints (64±4 MPa; 9.4±0.6 ksi) or those joints made with a Fe-29Ni-17Co spacer (41±11 MPa, 6±2 ksi). On average, 92% of the fracture path occurred within the Al_2O_3 material and 8% was along the Ag-Cu-Ti/Al_2O_3 interface.

The joints made at 900°C and 10 min were considerably weaker at 62±22 MPa (9±3 ksi); the fracture morphology was a mixture of cracking in the Al_2O_3 material (77%) as well as failure at the Ag-Cu-Ti/Al_2O_3 interface (23%).

It is interesting to note that nearly the same strength levels and failure morphologies were observed with the Co and Fe spacer for similar process conditions. Yet, the Fe spacer material resulted in significantly thicker Ti_xO_y reaction layers at the Ag-Cu-Ti/Al_2O_3 interface. Therefore, a comparison of pull test data for the Co and Fe spacers confirmed that the tensile strength of active metal joint strengths is not a monotonic function of the Ti_xO_y reaction layer thickness.

Ag-Cu-Ti Filler Metal Interactions with the Ni Spacer Material

Shown in Fig. 11A is an SEM (back-scattered electron) photograph of the joint formed with the Ni spacer, using the 850°C, 5-min process. Numerous particles were observed in the filler metal field having a diameter from 1 μm to 10 μm. In addition, a significant reaction layer 5 to 10 μm thick had developed at the Ag-Cu-Ti/Ni interface. Shown in Fig. 11B is an SEM photograph of the braze joint formed with the 900°C, 10-min process. In this case, the filler metal particles have generally smaller diameters. Also, a lace-work phase had developed. There was no evidence of a Ti_xO_y reaction layer at the

Ag-Cu-Ti/Al_2O_3 interface of either micrograph.

Shown in Fig. 12 is an EMPA trace made across the braze joint that was fabricated with the 850°C, 5-min process. The concentration profiles of Cu and Ag were those expected of the binary Ag-Cu eutectic composition. A total of 59 particles were recorded from all 14 EMPA traces. The particle phase could be separated into two composition groups as shown in Table 5. (There were no detectable levels of Al or Si.) The compositional distinction was the strength of Cu and Ag signals and the correspondingly inverse behaviors of the Ti and Ni signals. Coincidental with the compositional difference was a physical distinction; that is, group A had relatively larger particles and group B, smaller particles. The opposite trends of Cu and Ag signal strength vs. particle size suggested an X-ray sampling volume effect. The X-ray signal included more of the filler metal with the smaller particles of group B and, conversely, less of the filler metal with the larger particles of group A. The normalized proportions of Ni and Ti for both composition groups indicated a Ni_3Ti stoichiometry that is found in the Ni-Ti equilibrium phase diagram (Ref. 22).

The EMPA elemental profiles across braze joints made at 900°C for 10 min were similarly examined. The compositional data are also provided in Table 5. The *total* number of the particles examined was nearly the same as were evaluated with the reduced processing conditions. However, the 900°C, 10-min process resulted in a larger fraction of the smaller particles (phase composition group B, N = 51) than large particles (group A, N = 6). The phase compositions of both groups, when normalized between Ni and Ti, was Ni_3Ti.

The EMPA was performed across the Ag-Cu-Ti/Al_2O_3 interface. There was no evidence that a reaction layer was present there for either process condition.

The EMPA identified two sublayer phase compositions at the Ag-Cu-Ti/Ni interface resulting from the 850°C, 5-min process. These sublayers were indicated in Fig. 11A. The first sublayer, which was next to the Ag-Cu-Ti filler metal, exhibited a Ni_3Ti stoichiometry. The high Cu and Ag contents (36±25% and 15±16%, respectively) reflected the nearby filler metal. Aluminum was observed in only trace amounts. A second sublayer developed between the first sublayer and the Ni spacer having the composition 86±3 at-% Cu, 12±3 at-% Ni, and 1.9±0.5 at-% Ag. The equilibrium Cu-Ni binary system shows the two elements to exist as a complete solid-solution after solidification (Ref. 23). Therefore, this sublayer phase was a (Cu, Ni) solid-solution with a small amount of Ag. Silver has a finite, albeit limited, solubility in Cu. The (Cu, Ni) phase is not obvious in Fig. 11A or B because Ni and Cu have similar atomic numbers, which reduces the SEM contrast between the (Cu, Ni) phase and the pure Ni spacer.

Table 5 — Compositions of Particles in Braze Joints Made with Ni Spacer

Process Conditions		Elemental Concentrations (at-%) Ti	Cu	Ag	Ni
850°C, 5 min	A (N=22)	19 ± 2	15 ± 6	9 ± 6	57 ± 5
	B (N=37)	9 ± 4	30 ± 18	33 ± 22	28 ± 11
900°C, 10 min	A (N=6)	16 ± 3	18 ± 7	11 ± 4	54 ± 4
	B (N=51)	9 ± 4	30 ± 17	31 ± 19	31 ± 12

The 900°C, 10-min process also resulted in multiple sublayer phases at the Ag-Cu-Ti/Ni interface — Fig. 11B. A sublayer phase observed intermittently next to the filler metal was 6±9 at-% Ti, 45±11 at-% Ni, 26±14 at-% Cu, and 15±9 at-% Ag. The high concentration of Cu (relative to the filler metal nominal composition), together with Ni, suggested that the first sublayer was comprised of a Ni-rich, (Cu, Ni) solid-solution phase; and it was designated $(Cu, Ni)_a$. A second sublayer phase located adjacent to the Ni spacer was also a (Cu, Ni) solid-solution phase, but with a Cu-rich composition: 70±6%Cu, 27±5%Ni, and 2±2%Ag; it was designated $(Cu, Ni)_b$. This Cu-rich (Cu, Ni) solid-solution phase was higher in Ni than the corresponding Cu-rich, solid-solution phase observed after the 850°C, 5-min process. Again, Ag was present due to its limited solubility in Cu.

All tensile button braze joints were not hermetic, coinciding with the absence of a substantive Ti_xO_y reaction layer at the Ag-Cu-Ti/Al_2O_3 interface.

The pull strength of the Ni spacer braze joints made with the 850°C, 5-min process was 58±22 MPa (8±3 ksi). This value is similar to that of correspondingly processed Al_2O_3/Ag-Cu-Ti/Al_2O_3 joints (64±4 MPa; 9.4±0.6 ksi) and braze joints made with a Fe-29Ni-17Co spacer (41±11 MPa, 6±2 ksi). On average, 83% of the fracture path was at the Ag-Cu-Ti/Al_2O_3 interface and 17% of fracture occurred within the Al_2O_3. This fracture morphology differed from results with the Fe and Co spacers for which higher percentages of the fracture path was in the Al_2O_3 substrate.

The pull strengths were lower with the 900°C, 10-min process, being to 31±13 MPa (4±3 ksi). This strength was less than that of similarly processed braze joints using a Fe-29Ni-17Co spacer (53±14 MPa; 8±2 ksi). One hundred percent of the fracture paths were at the Ag-Cu-Ti/Al_2O_3 interface, again, in sharp contrast to the fracture behavior with the Fe and Co spacers.

Physical Metallurgy

A synopsis was made of the physical and metallurgical aspects of Ag-Cu-Ti braze joints made to Fe, Co, or Ni spacers. Those aspects were then correlated to the scavenging reaction observed between the Ag-Cu-Ti filler metal and the Fe-29Ni-17Co alloy. The synopses and a correlation between these and the original scavenging problem appear below.

1) Fe spacer: The reaction at the Ag-Cu-Ti/Fe interface produced several Fe_x-Ti_y-phase compositions. Those phases were either metastable or mixtures of known equilibrium compositions. The reaction was very limited, thereby allowing formation of a thick Ti_xO_y reaction layer at the Ag-Cu-Ti/Al_2O_3 interface. There was no significant presence of Fe in the filler metal.

2) Co spacer: A scavenging reaction formed a lacework phase that originated at the Ag-Cu-Ti/Co interface and then moved into the filler metal. Several Co_xTi_y compositions were observed after either process condition, which included the equilibrium Co_3Ti phase as well as metastable phases or mixtures of other equilibrium phases. In addition, the 900°C, 10-min process resulted in lacework phase composition of largely elemental Co. Formation of the Co_xTi_y lacework phase limited the Ti_xO_y reaction product at the Ag-Cu-Ti/Al_2O_3 interface to thin, intermittent layers.

3) Ni spacer: A significant Ni-Ti scavenging reaction occurred that included a reaction layer along the Ag-Cu-Ti/Ni interface as well as Ni_3Ti particles in the filler metal field. The Ag-Cu-Ti/Ni interface reaction products were Ni_3T and (Cu, Ni) solid-solution compositions. The distribution of Ni_3Ti phase particles suggested a precipitation process based upon dissolved Ni in the filler metal. The scavenging reactions left no significant Ti_xO_y reaction layer at the Ag-Cu-Ti/Al_2O_3 interface.

The above results suggest that the interaction between a Fe-29Ni-17Co spacer and the Ti component of the Ag-Cu-Ti

filler metal began as an interfacial reaction process as opposed to large-scale dissolution. The reaction layer at the Fe-29Ni-17Co/Ag-Cu-Ti interface was initially Fe-rich, due to the relatively high concentration of Fe in the alloy, and as such, remained attached to the Fe-29Ni-17Co spacer. Then, the Ni-Ti and Co-Ti reactions, more so the former, dominated layer development and were responsible for a large part of the scavenging of Ti. The layer thickened and then broke away from the spacer with the Ni-rich chemistry. An increased Cu content coincided with a higher Ni content due to (Cu, Ni) mutual solubility. The tendency for Ni from the base metal to dissolve and form Ni_3Ti particles was suppressed by the Fe and Co constituents, favoring rather the more contiguous lacework phase morphology.

Mechanical Metallurgy

The nominal pull strengths of the braze joints made with the Fe, Ni, or Co spacers were highest with the Fe and Co spacers. These strenghts exceeded that of the Fe-29Ni-17Co braze joints. The lowest were observed with the Ni spacer; the latter strengths were comparable to that of the Fe-29Ni-17Co braze joints. Also, lower joint strengths were observed for all spacer materials following the 900°C, 10-min process; these values were comparable to that of Fe-29Ni-17Co braze joints. (However, the individual strength rankings between Fe, Co, and Ni spacers remained unchanged.) In the case of braze joints made with the Fe-29Ni-17Co spacer, there was no significant difference in the braze joint strengths between the 850°, 5 min, and 900°, 10 min processes (41±11 MPa, 6±2 ksi; and 53±14 MPa, 8±2 ksi, respectively).

Two fracture modes were predominant. Those modes were 1) fracture within the Al_2O_3 substrate and 2) failure along the Ag-Cu-Ti/Al_2O_3 interface. Fracture was not observed at the Ag-Cu-Ti/X (X = Fe, Ni, Co) interface nor in the bulk filler metal, indicating that braze joint strength was insensitive to the different microstructures that formed at either location. Similar fracture morphology trends were observed for joints assembled with the Fe-29Ni-17Co spacer.

Based upon the above data, pull strength can only be correlated to the presence or absence of a Ti_xO_y reaction layer for braze joints made with either process. The absence of any reaction at the Ag-Cu-Ti/Al_2O_3 interface for the Ni spacer was accompanied by a significantly lower strength. Similar strengths resulted from Fe-29Ni-17Co spacers, which, likewise, did not allow a Ti_xO_y layer to develop. Both the Fe and Co spacers exhibited higher strengths, yet with vastly different Ti_xO_y thicknesses. The Fe spacer resulted in a larger data scatter.

Any significant impact by the Ti_xO_y layer thickness on joint strength appears to be further diminished by the fact that the 900°C, 10-min process caused a significant reduction in strength for all spacers, even joints made with the Ni spacer which did not produce a Ti_xO_y reaction layer at the Ag-Cu-Ti/Al_2O_3 interface. The concurrent increase in fracture at this interface certainly suggested a loss of strengh there that was not explicitly attributable to the Ti_xO_y layer. Rather, an alternative mechanism may provide contributing factors, including thermal expansion-induced damage and the effects of filler metal interlocking in the Al_2O_3 surface grains. Therefore, the strength levels of braze joints made with the Fe-29Ni-17Co spacers were commensurate with the absence of a Ti_xO_y layer. Mechanical attachment (interlocking) between the filler metal and the Al_2O_3 surface structure provided the nominal strengths of those joints and the joints made with the Ni interlayer.

Hermeticity

Hermeticity appears to have been directly dependent upon the extent of Ti_xO_y reaction layer growth at the Ag-Cu-Ti/Al_2O_3 interface. Therefore, the absence of a Ti_xO_y reaction layer in Ag-Cu-Ti braze joints made with the Fe-29Ni-17Co spacers was responsible for poor hermeticity performance.

Conclusions

1) Poor hermeticity performance was observed for Al_2O_3-Al_2O_3 braze joints having an Fe-29Ni-17Co alloy spacer and brazed with an Ag-Cu-Ti active filler metal. Satisfactory tensile strength was exhibited by the braze joints. Titanium was scavenged from the filler metal through formation of a (Fe, Ni, Co)-Ti lacework phase, thereby preventing formation of a Ti_xO_y reaction layer at the Ag-Cu-Ti/Al_2O_3 interface. The scavenging mechanism was further analyzed by examining braze joints made with elemental Fe, Ni, or Co spacers, and two brazing process conditions.

2) The Fe spacer caused the development of Fe_xTi_y phases at its interface with the Ag-Cu-Ti filler metal. Formation of a significant Ti_xO_y layer occurred at the Ag-Cu-Ti/Al_2O_3 interface resulting in 100% of the braze joints being hermetic.

3) The Co spacer resulted in the development of a lacework phase having the Co_3Ti and potentially metastable Co_xTi_y compositions. A thin, intermittent Ti_xO_y reaction layer was observed at the Ag-Cu-Ti/Al_2O_3 interface resulting in only 75% of the buttons being hermetic.

4) The Ni spacer caused an extensive Ni_3Ti phase to form at the Ag-Cu-Ti/Ni interface as well as discrete Ni_3Ti phase particles to develop in the filler metal. A (Cu, Ni) solid-solution phase was also observed at the Ni spacer interface. Complete scavenging of Ti resulted in the absence of a Ti_xO_y layer at the Ag-Cu-Ti/Al_2O_3 interface. Zero percent of the braze joints were hermetic.

5) The pull strengths of the braze joints correlated primarily with the presence or absence of the Ti_xO_y layer; there was no strong dependence on the thickness of the Ti_xO_y layer. Higher strength values were observed with the 850°C, 5-min process. The fracture path was primarily in the Al_2O_3 substrate. Lower strengths produced by the 900°C, 10-min process were accompanied by increased fracture along the Ag-Cu-Ti/Al_2O_3 interface.

6) The Fe, Ni, and Co spacer experiments suggested that the lacework phase that formed in Fe-29Ni-17Co/Ag-Cu-Ti couples began as an interfacial reaction. An Fe-rich phase developed adjacent to the spacer, but with very limited Ti scavenging. However, further growth became dominated by the Ni and Co components of the spacer, which significantly scavenged Ti from the filler metal. The Ni-rich reaction layer separated from the spacer surface and entered the filler metal field with the lacework morphology. Pull strength, fracture morphology, and poor hermeticity were all commensurate with the absence of a Ti_xO_y reaction layer at the Ag-Cu-Ti/Al_2O_3 interface.

7) This study indicates that the application of a barrier layer on the Fe-29Ni-17Co alloy, in particular, elemental Fe, or other nonreactive metal (e.g., Mo), would curtail the Ti scavenging reaction.

Acknowledgments

The authors wish to thank A. Kilgo, Garry Bryant, and Drew Leach, who performed the metallographic sample preparation and provided the optical micrographs, as well as Charlie Robino for his detailed review of the manuscript. This work was supported by the Dept. of Energy under contract DE-AC04-94AL8500. Sandia is a multiprogram laboratory operated by Sandia Corp., a Lockheed Martin Co., for the U.S. Dept. of Energy.

References

1. Mangin, C., Neely, J., and Clark, J. 1993. The potential for advanced ceramics in automotive engine applications. *Journal of Metals* (6): 23–27.

2. Signliano, R., and Lanzone, R. 1996. Multilayer ceramics: a revitalization. *Elect. Pack. and Prod*. (9): 47–51.

3. Okamura, H. 1993. Brazing ceramics and metals. *Welding Inter.* 7(3): 236–242.

4. Levy, A. 1991. Thermal residual stresses in ceramic-to-metal brazed joints. *Journal American Ceramics Society* 74(9): 2141–2147.

5. Kovar™ is a registered trademark of Carpenter Technologies Corp. The spacer material used in these assemblies was designated as ASTM F186 and is often referred to as "clean" Kovar™.

6. Moorhead, A., and Hyour, K. 1992. Joining oxide ceramics. *Eng. Mater. Handbook*, Vol. 4, Ceramics and Glasses. pp. 511–522. Materials Park, Ohio.: ASM International.

7. Cusil ABA™ is a registered trademark of Wesgo Industries.

8. Hahn, S., Kim, M., and Kang, S. 1998. A study of the reliability of brazed Al_2O_3 joint systems. IEEE Trans. on *Components, Packaging and Manufacturing Technology* 21: 211–216.

9. Inconel is a registered trademark of INCO, International.

10. Wielage, B., Podlesak, H., and Klose, H. 1997. Reaction layer formation on the metal side of active brazed, metal-ceramic joints. *Proc. Joining 97 Conference*, Jena, Germany.

11. AL500™ is a tradename for the Al_2O_3 produced by Wesgo Industries.

12. Moorhead, A., et al. 1988. The role of interfacial reactions on the mechanical properties of ceramic brazements. *Ceramic Microstructures '86,* eds. J. Pask and A. Evans, pp. 949–958. New York, N.Y.: Plenum Press.

13. Bang, K., and Liu, S. 1994. Interfacial reaction between alumina and Cu-Ti filler metal during reactive metal brazing, *Welding Journal* 73(3): 54-s to 60-s.

14. *Binary Alloy Phase Diagrams*. 1986. Ed. T. Massalski, pp. 25, 915. Materials Park, Ohio: ASM International.

15. Ibid, p. 1118.

16. Haimovich, J., and Kahn, D. 1990. Metastable nickel-tin intermetallic compound in tin-based coatings. *Proceedings of the 77th AESF Annual Technical Conference* pp. 689–712, Association of Electroplaters and Surface Finishers.

17. Vianco, P., Kilgo, A., and Grant, R. 1995. Intermetallic compound layer growth by solid-state reactions between 58Bi-42Sn solder and copper. *Journal of Electronic Materials* 24: 1493–1505.

18. Vianco, P., Kilgo, A., and Grant, R. 1995. Solid-state intermetallic compound layer growth between copper and hot dipped indium coatings. *Journal of Materials Science* 30: 4871–4878.

19. Scott, P., et al. 1975. The wetting and bonding of diamonds by copper-base binary alloys. *Journal of Materials Science* 10: 1833–1840.

20. *Binary Alloy Phase Diagrams.* 1986. Ed. T. Massalski, p. 809. Materials Park, Ohio: ASM International.

21 Kubaschewski, O., and Evans, E. 1956. *Metallurgical Thermochemistry*. London, U.K.: Pergamon Press. pp. 331–338.

22. *Binary Alloy Phase Diagrams.* 1986. Ed. T. Massalski, p. 1768. Materials Park, Ohio: ASM International,

23. Ibid., p. 942.

2004 Poster Session Call for Entries

The American Welding Society announces a Call for Entries for the 2004 Poster Session to be held as part of Welding Show 2004 on April 6–8, 2004, in Chicago, Ill. Students, educators, researchers, engineers, technical committees, consultants, and anyone else in a welding- or joining-related field are invited to participate in the world's leading annual welding event by visually displaying their technical accomplishments in a brief graphic presentation, suitable for close, first-hand examination by interested individuals.

Posters provide an ideal format to present results that are best communicated visually, more suited for display than verbal presentation before a large audience; new techniques or procedures that are best discussed in detail individually with interested viewers; brief reports on work in progress; and results that call for the close study of photomicrographs or other illustrative materials.

Submissions should fall into one of the following two categories and will be accepted only in a specific format. Individuals interested in participating should contact Dorcas Troche, Manager, Conferences & Seminars, via e-mail at *dorcas@aws.org* for specific details. Deadline for submission of entries is Monday, December 1, 2003.

1. Student Division
   - ∞Category A: 2-Year or Certificate Program
   - ∞Category B: Undergraduate Degree
   - ∞Category C: Graduate Degree

2. Professional/Commercial Division